

# [( $\equiv$ SiO)Ta<sup>V</sup>Cl<sub>2</sub>Me<sub>2</sub>]: A Well-Defined Silica-Supported Tantalum(V) Surface Complex as Catalyst Precursor for the Selective Cocatalyst-Free Trimerization of Ethylene\*\*

Yin Chen, Emmanuel Callens, Edy Abou-Hamad, Nicolas Merle, Andrew J. P. White, Mostafa Taoufik, Christophe Copéret, Erwan Le Roux,\* and Jean-Marie Basset\*

Over the last 50 years, the production of linear  $\alpha$ -olefins by ethylene oligomerization has gained increasing interest in industrial and academic research.<sup>[1,2]</sup> Currently, numerous studies in this field have been reported and developed into industrial processes: titanium-based catalysts for the dimerization of ethylene (Alpha-butol, IFP);<sup>[3]</sup> chromium-based catalysts for the trimerization of ethylene (Phillips Petroleum),<sup>[4]</sup> and more recently chromium-bearing PNP ligand for ethylene tetramerization (SASOL).<sup>[5]</sup> Along with these now-classical systems, which require co-catalysts such as MAO, Sen also reported the use of tantalum pentachloride in combination with an alkylating agent, such as SnMe<sub>4</sub>, ZnMe<sub>2</sub>, AlMe<sub>3</sub>, or MeLi. In this case, the catalysts is assumed to be Ta<sup>III</sup> species formed in situ by the reduction of TaMe<sub>2</sub>Cl<sub>3</sub> in the presence of ethylene.<sup>[6]</sup> In this context, Mashima and co-workers have shown that Ta<sup>III</sup> active species can be alternatively formed by reduction of Ta<sup>V</sup>Cl<sub>5</sub> by 3,6-bis(trimethylsilyl)-1,4-cyclohexadiene derivatives.<sup>[7]</sup> However the catalytic performances of these systems require the addition of co-catalysts. In several instances, site isolation on the oxide surface has been highly beneficial to the design of efficient catalysts, compared to inactive or rapidly deactivating molec-

ular analogues, which is in particular due to the absence of bimolecular reactions between supported metal complexes.<sup>[8]</sup> When considering the reaction intermediates, and in the view of developing well-defined silica supported species, we targeted the immobilization of Me<sub>3</sub>TaCl<sub>2</sub><sup>[9]</sup> onto an inorganic carrier, silica, by surface organometallic chemistry (SOMC) as a catalyst precursor.

Herein, we report the synthesis and the surface characterization of the grafted organometallic species ( $\equiv$ SiO)-Ta<sup>V</sup>Cl<sub>2</sub>Me<sub>2</sub> **2** in view of its application in ethylene oligomerization. Furthermore, mechanistic studies on this selective catalytic process have been successfully achieved thanks to the dynamic reactor used. They indicate three different pathways for the initiation process.

SBA-15 was selected because of its ordered mesoporous network with large surface area (Supporting Information, Figures S1, S2).<sup>[10]</sup> This porous silica was subjected to partial dehydroxylation under vacuum at 700 °C to afford SBA-15<sub>(700)</sub>, which features mostly isolated silanols, as indicated on the IR spectrum by the characteristic sharp peak at 3747 cm<sup>-1</sup> (Supporting Information, Figure S3). SBA-15<sub>(700)</sub> was reacted with TaCl<sub>2</sub>Me<sub>3</sub> **1** (Supporting Information, Figure S4), and the resulting powder was characterized to determine the organometallic species on the surface prior to its catalytic application.<sup>[11]</sup> Elemental analysis gave 14.8 % Ta, 1.65 % C, and 0.39 % H, with a ratio of Ta/C/Cl = 1:1.97:1.88 (theoretical: Ta/C/Cl = 1:2:2).

<sup>1</sup>H-MAS NMR spectrum of **2** unexpectedly displays two major signals at 1.27 ppm and 0.85 ppm with a broad peak at 1.90 ppm and a very weak signal at -0.03 ppm, which is probably due to methane or a trace amount of  $\equiv$ SiMe (see below for further comments, and the Supporting Information, Figure S5). The NMR signal at 1.9 ppm most likely corresponds to the small amount of unreacted silanols, in agreement with IR spectroscopy results. Two peaks appear at 1.27 and 0.85 ppm that would be consistent with two inequivalent methyl groups coming from one species or indicating the presence of two distinct species.

Proton double (DQ)- and triple (TQ)-quantum correlation spectra under 22 kHz MAS (Supporting Information, Figure S6) confirm that these two signals correspond to methyl groups, most likely from two different species in view of the absence of correlation of diagonal peak.<sup>[12]</sup> Autocorrelation peaks are observed on the diagonal of the 2D DQ spectrum for all the protons (notably, this shows that unreacted silanols are in close proximity to each other and most likely located in micropores). A strong autocorrelation

[\*] Y. Chen, E. Callens, E. Abou-Hamad, J.-M. Basset  
KAUST Catalysis Center  
King Abdullah University of Science and Technology  
Thuwal 23955-6900 (Kingdom of Saudi Arabia)  
E-mail: jeanmarie.basset@kaust.edu.sa

N. Merle, M. Taoufik, C. Copéret  
Chimie Organometallique de Surface/Laboratoire de Chimie,  
Polymères et Procédés UMR-C2P2-5265CNRS/ESCPE-Lyon/UCBL  
ESCPE Lyon  
F-308-43 Boulevard du 11 Novembre 1918  
F-69616, Villeurbanne Cedex (France)

A. J. P. White  
Department of Chemistry, Imperial College London  
Exhibition Road, London SW7 2AZ, England (UK)

E. Le Roux  
Department of Chemistry, University of Bergen  
Realfagbygget, Allegaten 41, 5007, Bergen (Norway)  
E-mail: Erwan.leRoux@kj.uib.no

C. Copéret  
Department of Chemistry, ETH Zurich  
HCI H 229 Wolfgang-Pauli-Strasse 10, 8093, Zurich (Switzerland)

[\*\*] We are indebted to Prof. Lyndon Emsley for his enthusiastic discussion and suggestions. The work is supported by KAUST and SABIC.

Supporting information for this article is available on the WWW under <http://dx.doi.org/10.1002/anie.201206272>.

peak is observed in the TQ spectrum for both resonances attributed to methyl groups (0.85, 1.27 in F2 and 2.55, 3.81 ppm in F1). As expected, the silanols do not show a TQ correlation. To obtain a better assignment of the structure of the supported Ta species, a series of NMR spectroscopy experiments have been performed, and two batches of  $^{13}\text{C}$ -enriched  $\text{TaCl}_2(^{13}\text{CH}_3)_3$  **1**\* (at 19% and 97%) onto SBA-15<sub>(700)</sub> were synthesized. The  $^{13}\text{C}$  CP/MAS NMR spectrum of **2** displays two peaks at 61 ppm and 67 ppm (Figure 1a), quantitative  $^{13}\text{C}$  NMR MAS gives a ratio of these two peaks of 1:2 (Supporting Information, Figure S8).

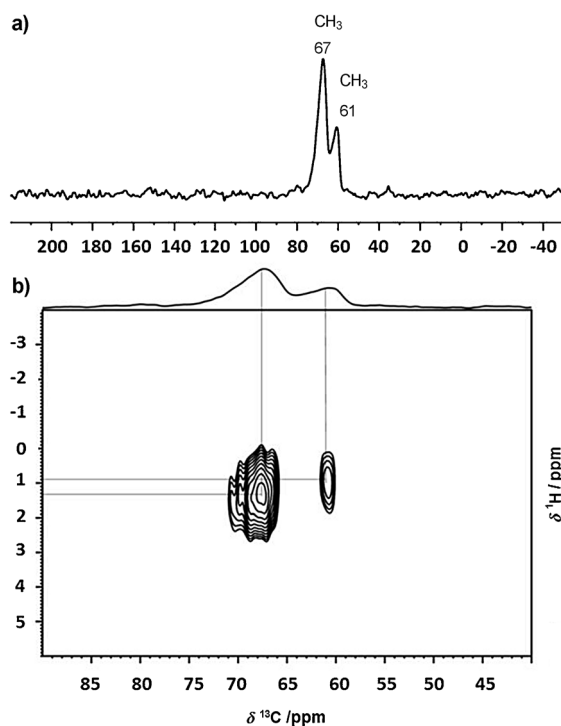
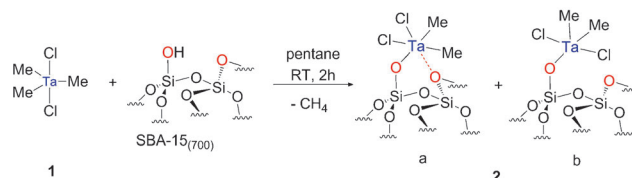


**Figure 1.** 1D  $^{13}\text{C}$  PMAS spectrum (a) and contour plot (b) of the aliphatic region of a  $^1\text{H}$ – $^{13}\text{C}$  HETCOR spectrum of  $(\equiv\text{SiO})\text{Ta}^{\text{V}}\text{Cl}_2\text{Me}_2$  recorded with a contact time of 0.5 ms. (Experimental details are given in the Supporting Information.)

The 2D HETCOR spectrum with short contact time (0.5 ms) shows a clear correlation between the methyl protons and these two carbon atoms, allowing the assignment of the carbon–proton pairs to the individual methyl groups (Figure 1). Long-range 2D HETCOR with contact times between 0.5 and 8 ms shows no additional correlation peaks arising from longer-range dipolar through-space interactions (Supporting Information, Figure S9a), confirming that these two peaks correspond to two different species. When a very long contact time was employed (10 ms), these peaks start to correlate, suggesting the proximity of some of the species (Supporting Information, Figure S9b). Moreover, grafting a varying amount of  $[\text{TaCl}_2(^{13}\text{CH}_3)_3]$  **1**\* per surface silanol (25/50/98% coverage) provided further evidence for the presence of two distinct species. At low coverage, the peak at 61 ppm has a greater intensity than the peak at 67 ppm in the  $^{13}\text{C}$  NMR spectrum, while the situation is reverse at high

coverage. This confirms the presence of two surface species, possibly resulting from grafting on isolated silanols of different environment and reactivity (Supporting Information, Figure S10).<sup>[13]</sup> In fact, a CP/Static  $^{13}\text{C}$  NMR spectrum reveals that these two methyl groups have different dynamics: the peak at 67 ppm is much broader and is associated with slower dynamics than the other at 61 ppm (Supporting Information, Figure S11). This indicates that the former probably interact more strongly with adjacent siloxane bridges and can be depicted as **2a** (Scheme 1). Variable-temperature experi-



**Scheme 1.** Synthesis of  $(\equiv\text{SiO})\text{Ta}^{\text{V}}\text{Cl}_2\text{Me}_2$  **2**.

ments of  $^{13}\text{C}$  CP/MAS NMR, with a temperature increasing from room temperature to 160 °C further support this interpretation: a new peak at –2 ppm, attributed to methane (decomposition of **1**) and  $\equiv\text{Si}$ –Me, resulting from a methyl transfer to the surface, appears at the expense of the decrease of intensity of the peak at 67 ppm (Supporting Information, Figure S12), while that at 61 ppm remains intact.

The species **2a** associated with the signal at 67 ppm most likely reacts with adjacent siloxane bridges (Supporting Information, Scheme S1). These results are in agreement with the presence of two species differing by the presence (**2a**) or not of adjacent siloxane bridges (**2b**) (Scheme 1).<sup>[13,14]</sup>

After extensive solid-state NMR studies to establish the structure of the grafted organometallic species, the activity of catalyst **2** for ethylene oligomerization was first investigated in a semi-batch autoclave in the liquid phase (Table 1). Under these conditions, this supported catalyst **2** is active for the ethylene oligomerization without co-catalysts or additives, with comparable productivity for 1-hexene as compared to the homogenous system.<sup>[6]</sup> Increasing the temperature to 100 °C gave the best productivity of 1-hexene, TON 375

**Table 1:** Oligomerization of ethylene catalyzed with **2**.

| Entry <sup>[a]</sup> | Pressure (bar) | T [°C] | 1-Butene [wt %] <sup>[b]</sup> | 1-Hexene [wt %] <sup>[c,d]</sup> | Activity <sup>[e]</sup> |
|----------------------|----------------|--------|--------------------------------|----------------------------------|-------------------------|
| 1                    | 50             | 60     | 6.0                            | 88.3 (98.1)                      | 160                     |
| 2                    | 50             | 70     | 5.4                            | 82.6 (98.8)                      | 242                     |
| 3                    | 50             | 80     | 5.9                            | 84.3 (99.2)                      | 322                     |
| 4                    | 50             | 90     | 7.3                            | 83.8 (99.0)                      | 332                     |
| 5                    | 50             | 100    | 9.6                            | 82.7 (99.1)                      | 375                     |
| 6                    | 50             | 110    | 7.8                            | 82.6 (99.3)                      | 273                     |
| 7                    | 40             | 100    | 7.1                            | 83.1 (97.7)                      | 270                     |
| 8                    | 30             | 100    | 11.1                           | 80.5 (97.6)                      | 200                     |
| 9                    | 20             | 100    | 7.3                            | 77.8 (97.1)                      | 148                     |

[a] Reaction conditions: 50 mg of **2**, 10 mL of toluene, 30 min. [b] Only 1-butene was detected. [c] Selectivity of 1-hexene in products. [d] Values in parentheses are selectivity in 1-hexene from  $\text{C}_6$ . [e] Turnovers mol(ethylene)/mol(Ta)/h.

(58 g<sub>1-hexene</sub>/g<sub>Ta</sub> h) at an optimal pressure of 50 bar of ethylene (Table 1, entries 1–5 and 7–10; Supporting Information, Figure S13). Performing the catalytic test at 110 °C led to a decrease of productivity (Table 1, entry 6).

Moreover, the productivity for 1-hexene is linearly correlated to the pressure of ethylene indicating a first-order reaction (Supporting Information, Figure S14, Scheme S2). The major oligomer produced is 1-hexene (> 80 %) along with 1-butene (< 10 %) and polyethylene. Solid-state NMR analysis of the residual catalyst at the end of the reaction showed mainly polyethylene, which may be the cause of the catalyst ageing (Supporting Information, Figure S15).

Previous results postulated Ta<sup>III</sup> intermediates, which leads, via oxidative coupling of ethylene, to tantalacyclopentane(V), a key intermediate for the oligomerization reaction.<sup>[6,7]</sup> However, to date, there is no direct evidence for the formation of this intermediate. Therefore, we investigated the conversion of Ta<sup>V</sup> precursor into the active species using a dynamic bed reactor coupled with a GC detector in situ to monitor this reduction step closely.

Contacting **2** with ethylene (12 bar, 0.42 mL min<sup>-1</sup>, ca. 0.18 mol of ethylene/mol·Ta·min) at 70 °C in a flow bed reactor gave with time a mixture of methane, propylene, ethane, and butane resulting from a reductive elimination step (Figure 2). Within 150 min, dimerization of ethylene

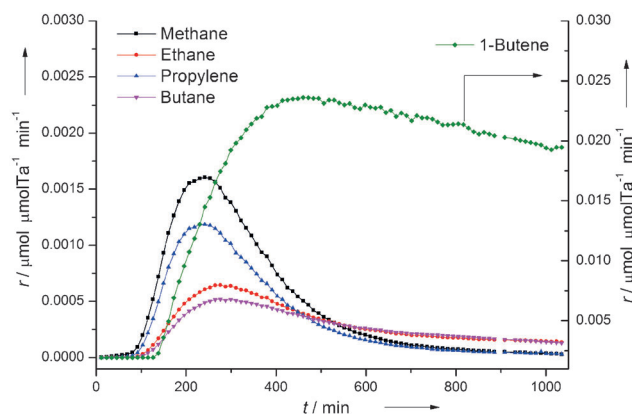
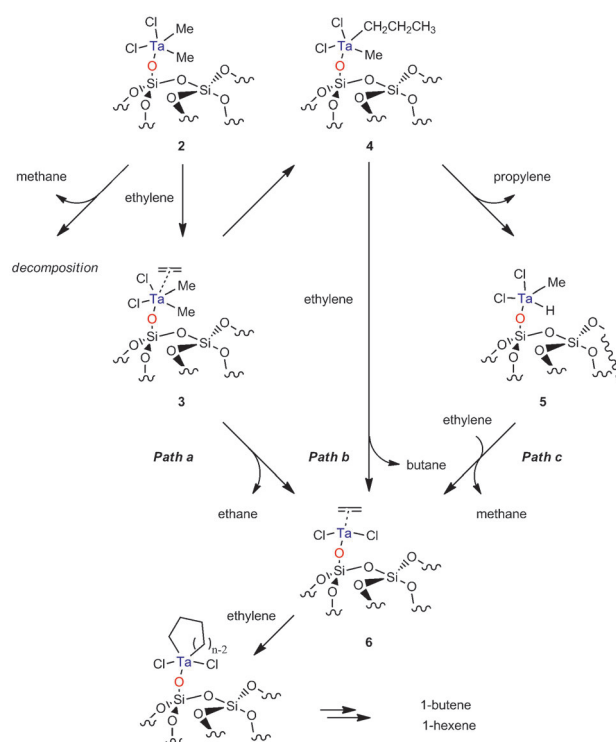


**Figure 2.** Initial products observed of the reaction of **2** with ethylene in a dynamic reactor.

started and gave mainly 1-butene and traces of 1-hexene in flow conditions. After 450 min the activation process was nearly finished, and the generation of these four gases stopped. Moreover, the catalyst produces 1-butene as the major product during an extended period. After 5000 min, 110 mol of butene per mol Ta atom were produced (Supporting Information, Figure S16). All four gases observed in the activation process are consistent with the formation of an Ta<sup>(III)</sup> intermediate species through competitive pathways (Scheme 2). The process probably starts with the coordination of ethylene; it can insert into the Ta–Me bond to generate **4**, which by a  $\beta$ -hydrogen elimination produce first **5** and then **6** via a subsequent reductive elimination of methane (path c).<sup>[6]</sup> We also observed ethane and butane, which are presumably formed by reductive elimination from the inter-



**Scheme 2.** Proposed mechanism pathways for the formation of butane, ethane, methane, propylene, and active Ta<sup>III</sup> surface species.

mediate **3** (path a) and **4** (path b) respectively, and which also leads to **6**.

Additionally, analysis of the quantity of the four gases formed during activation (up to 1050 min) showed that butane/ethane/propylene were generated in a 1/1.11/1.33 ratio by three competitive pathways, and the amount of products (52.1  $\mu$ mol of CH<sub>4</sub>, 38.6  $\mu$ mol of propylene, 32.0  $\mu$ mol of C<sub>2</sub>H<sub>6</sub>, and 28.9  $\mu$ mol of butane, accordingly, the methane generated from deactivation pathway and ethylene disproportionation pathway has a ratio around 1:3) with respect to Ta (110.9  $\mu$ mol) shows that about 90 % of Ta<sup>V</sup> species have been converted into active species **6** (Supporting Information, Figure S17 and S18). This species is converted, in the presence of ethylene, into the key putative tantalacycle intermediates, which finally yields 1-alkenes, that is, 1-butene and 1-hexene in gas versus condensed-phase conditions.<sup>[6b]</sup>

In conclusion, a supported catalyst for the ethylene oligomerization has been designed by a molecular approach; it operates efficiently without co-catalyst delivering 1-hexene in good selectivity in a liquid phase and 1-butene in a gas phase. The use of a well-defined catalyst precursor ( $(\equiv\text{SiO})\text{Ta}^{\text{V}}\text{Cl}_2\text{Me}_2$ ) and monitoring the initiation products show clearly that ethylene initially converts the Ta<sup>V</sup> catalyst precursor into the formally reduced Ta<sup>III</sup>, which can then generate the key metallacycle intermediates, and thus the selective production of  $\alpha$ -olefins.

Received: August 5, 2012

Published online: October 22, 2012

**Keywords:** ethylene · oligomerization · organometallic compounds · surface reactions · tantalum

- [1] a) D. S. McGuinness, *Chem. Rev.* **2011**, *111*, 2321–2341; b) T. Agapie, *Coord. Chem. Rev.* **2011**, *255*, 861–880; c) P. W. N. M. van Leeuwen, N. D. Clément, M. J.-L. Tschan, *Coord. Chem. Rev.* **2011**, *255*, 1499–1517; d) J. Skupinska, *Chem. Rev.* **1991**, *91*, 613–648; e) H. Wittcoff, B. G. Reuben, J. S. Plotkin, *Industrial Organic Chemicals*, 2<sup>nd</sup> ed., Wiley-Interscience, New York, **2004**.
- [2] Y. Shaikh, K. Albahily, M. Sutcliffe, V. Fomitcheva, S. Gambartotta, I. Korobkov, R. Duchateau, *Angew. Chem.* **2012**, *124*, 1395–1398; *Angew. Chem. Int. Ed.* **2012**, *51*, 1366–1369.
- [3] a) Y. Chauvin, D. Commereuc, Y. Glaize (IFP), European Patent No. 0200654, **1989**; b) D. Commereuc, J. Gaillard, G. Leger (IFP), French Patent No. 2540488, **1984**; c) K. Ziegler, H. Martin, U.S. Patent 2943125, **1960**.
- [4] a) W. K. Reagen, B. K. Conroy (Phillips Petroleum), EP 416403, **1990**; b) J. T. Dixon, M. J. Green, F. M. Hess, D. H. Morgan, *J. Organomet. Chem.* **2004**, *689*, 3641–3668; c) J. R. Briggs (Union Carbide), U.S. Patent 4,668,838, **1987**; d) M. Tamura, K. Iwanaga, Y. Ito (Sumitomo Chemical), EP 699 648, **1995**; e) A. Carter, S. A. Cohen, N. A. Cooley, A. Murphy, J. Scutt, D. F. Wass, *Chem. Commun.* **2002**, 858–859.
- [5] a) K. Blann, A. Bollmann, J. T. Dixon, A. Neveling, D. H. Morgan, H. Maumela, E. Killian, F. Hess, S. Otto, L. Pepler, H. Mahomed, M. Overett (Sasol Technology), WO Patent 04056479A1, **2004**; b) A. H. Tullo, *Chem. Eng. News* **2005**, *83*(43), 30–33; c) A. Bollmann, K. Blann, J. T. Dixon, F. M. Hess, E. Killian, H. Maumela, D. S. McGuinness, D. H. Morgan, A. Neveling, S. Otto, M. Overett, A. M. Z. Slawin, P. Wasserscheid, S. Kuhlmann, *J. Am. Chem. Soc.* **2004**, *126*, 14712–14713; d) D. S. McGuinness, A. J. Rucklidge, R. P. Tooze, A. M. Z. Slawin, *Organometallics* **2007**, *26*, 2561–2569.
- [6] a) C. Andes, S. B. Harkins, S. Murtuza, K. Oyler, A. Sen, *J. Am. Chem. Soc.* **2001**, *123*, 7423–7424; b) Z.-X. Yu, K. N. Houk, *Angew. Chem.* **2003**, *115*, 832–835; *Angew. Chem. Int. Ed.* **2003**, *42*, 808–811.
- [7] a) R. Arteaga-Müller, H. Tsurugi, T. Saito, M. Yanagawa, S. Oda, K. Mashima, *J. Am. Chem. Soc.* **2009**, *131*, 5370–5371; b) M. Yanagawa, S. Oda, K. Mashima (Sumitomo Chemical Co), JP 2006/051489 (WO Patent 2006/006433), **2006**.
- [8] a) J.-M. Basset, R. Psaro, D. Roberto, R. Ugo, *Modern Surface Organometallic Chemistry*, Wiley-VCH, Weinheim, **2009**; b) C. Copéret, *Chem. Rev.* **2010**, *110*, 656–680; c) S. L. Wegener, T. J. Marks, P. C. Stair, *Acc. Chem. Res.* **2012**, *45*, 206–214, and references therein.
- [9] a) P. R. Sharp, D. Astruc, R. R. Schrock, *J. Organomet. Chem.* **1979**, *182*, 477–510; b) R. R. Schrock, G. W. Parshall, *Chem. Rev.* **1976**, *76*, 243–368; c) R. R. Schrock, *J. Organomet. Chem.* **1976**, *122*, 209–225; d) R. R. Schrock, P. R. Sharp, *J. Am. Chem. Soc.* **1978**, *100*, 2389–2399; e) R. R. Schrock, L. W. Messerle, C. D. Wood, L. J. Guggenberger, *J. Am. Chem. Soc.* **1978**, *100*, 3793–3800; f) R. R. Schrock, J. D. Fellmann, *J. Am. Chem. Soc.* **1978**, *100*, 3359–3370; g) R. R. Schrock, *Acc. Chem. Res.* **1979**, *12*, 98–104; h) R. R. Schrock, *J. Am. Chem. Soc.* **1974**, *96*, 6796–6797.
- [10] a) R. Anwander, *Chem. Mater.* **2001**, *13*, 4419–4438; b) C. Copéret, M. Chabanas, R. Petroff Saint-Arroman, J.-M. Basset, *Angew. Chem.* **2003**, *115*, 164–191; *Angew. Chem. Int. Ed.* **2003**, *42*, 156–181.
- [11] The structure of **1** was found to be similar as that previously reported by Sattler et al. The complex has crystallographic  $D_{3h}$  symmetry about an axis that passes through Cl1 and Ta1. As a consequence of this symmetry, the Cl–Ta–Cl, C–Ta–C, and Cl–Ta–C angles are exactly 180, 120 and 90°, respectively. See: A. Sattler, S. Ruccolo, G. Parkin, *Dalton Trans.* **2011**, *40*, 7777–7782.
- [12] H. Geen, J. J. Titman, J. Gottwald, H. W. Spiess, *Chem. Phys. Lett.* **1994**, *227*, 79–86.
- [13] a) M. Taoufik, A. de Mallmann, E. Prouzet, G. Saggio, J. Thivolle-Cazat, J.-M. Basset, *Organometallics* **2001**, *20*, 5518–5521; b) D. Gajan, C. Copéret, *New J. Chem.* **2011**, *35*, 2403–2408.
- [14] Methyl transfer from metal to silicon has already been observed when grafting silica dehydroxylated at high temperature (700 °C) and having strained siloxane bridges (metal–methyl, Groups 4 and 5). See: H. Ahn, T. J. Marks, *J. Am. Chem. Soc.* **2002**, *124*, 7103–7110.